Earth and Planetary Science
https://ojs.nassg.org/index.php/eps

RESEARCH ARTICLE

Curie Depth and Surface Heat Flow Estimation from Anomalous Magnetic Blocks in the Lower and Part of Middle Benue Trough and Anambra Basin

Mukaila Abdullahi[1*] **Yunis B. Valdon**[2] **Fartisincha P. Andrew**[1] **Bello Yusuf Idi**[1]

1. Department of Science Laboratory Technology, Modibbo Adama University, P.M.B. 2076, Yola, Nigeria
2. Department of Geology, Modibbo Adama University, P.M.B. 2076, Yola, Nigeria

ARTICLE INFO

Article history
Received: 28 February 2023
Revised: 7 April 2023
Accepted: 18 April 2023
Published Online: 23 April 2023

Keywords:
Curie depth
Surface heat flow
Geothermal energy
Magnetic data
Benue trough

ABSTRACT

Estimation of the bottom (Curie) depths and SHF values on blocks (A, B, C, …, Y) of magnetic anomalies in the lower and part of the middle Benue trough and Anambra basin have been presented. A Map of the result shows a shallow Curie depth of about 11 km around the area of Abakaliki with the deepest Curie depth of about 27 km obtained around Utukpa region. The overriding bottom (Curie) depth of 18 km is calculated around Iku mbur, Arufu and Igumale regions. Heat flow has also been calculated from the Curie depth results. The SHF vary from 54 mWm^{-2} around Utukpa to the highest value of 132 mWm^{-2} around Abakaliki. The obtained high SHF value could be of sufficiently good prospects for the exploration of geothermal energy resources in the region.

1. Introduction

Thermal anomaly is a manifestation of renewable and environmentally benign green geothermal energy resources. Geothermal studies are carried out based on magnetic anomaly [1-10]. Curie point depth/Curie depth is the point depth at which the magnetic sources at a particular geographic location within the Earth's crust lose their magnetism contents completely at a specific temperature known as the Curie point temperature [11].

The Curie (magnetic bottom) depths are often derived and computed from magnetic anomalies on the basis of spectral analysis [2,8-10,12-19]. Modification of the conventional spectral method was made for a robustly new method

*Corresponding Author:
Mukaila Abdullahi,
Department of Science Laboratory Technology, Modibbo Adama University, P.M.B. 2076, Yola, Nigeria;
Email: mukailaa.agp@mau.edu.ng

DOI: http://dx.doi.org/10.36956/eps.v2i1.821

called 'the centroid method' as presented [8,10,20,21].

Whereas, Surface Heat Flow (SHF) is the movement of heat energy from the interior part of the Earth to the surface. It can generally be estimated from the Curie depths using 1-D Fourier law based on heat transfer through conduction mode [2]. The process happens during the cooling of the Earth's core and the generation of radiogenic heat energy between 20 km and 40 km of the Earth's upper crust [19]. SHF is usually higher in the areas of high tectonic activity and thinner Earth's crust [19].

The Nigerian Benue trough despite a number of quantitative geothermal research based on magnetic anomalies in the region [20,22-27], which suggested Curie depths between 11 km and 33 km, SHF values between 51 mWm^{-2} and 132 mWm^{-2}, there are still more to be interpreted about the geodynamic process of the region in terms of these values.

In the present study therefore, the computed Curie depths using modified centroid method were used in the calculation of SHF using 1-D Fourier's law in the study region.

2. Geological Formations and Tectonics of the Region

The Benue trough (Figure 1) is a mega rifted system for many forms of Earth sciences research [28-37]. The sedimentary rocks beneath the region under study are the Asu River Group, which comprises Albian marine shales and limestones with sandstone intercalations that formed the oldest formation beneath the region.

Asu River Group is observed around the areas of Abakaliki, Iku mbur, Ugba, Oturkpo and somewhere around the east of Ebeel area (Figure 2). The Cenomanian-Turonian Eze-Aku formation consists of the blackshales, siltstones and calcareous sandstones. The Awgu formation is a coal-bearing formation of the Late Turonian-Early Santonian. The Nkporo formation comprises the shales and mudstone of the Coniacian/Maestrichtian depositional cycle. Exposure of Nkporo formation is observed around the village of Otukpa area of Enugu (Figure 2). Bassange formation is composed of the sandstones and ironstones, which are also of the Coniacian/Maestrichtian depositional cycle. This formation (Bassange) is sandwiched between the Nkporo and Awgu shales (Figure 2). The lower coal formation comprising coal, sandstones and shales is overlain by the Nkporo formations in the Anambra basin. The Nsukka formation comprises the false-bedded sandstones that mark yet another transgression in the Anambra basin during the Paleocene [34,35]. Understanding the basement setup on the basis of gravity and magnetic anomalies in the region has been reported [36-39].

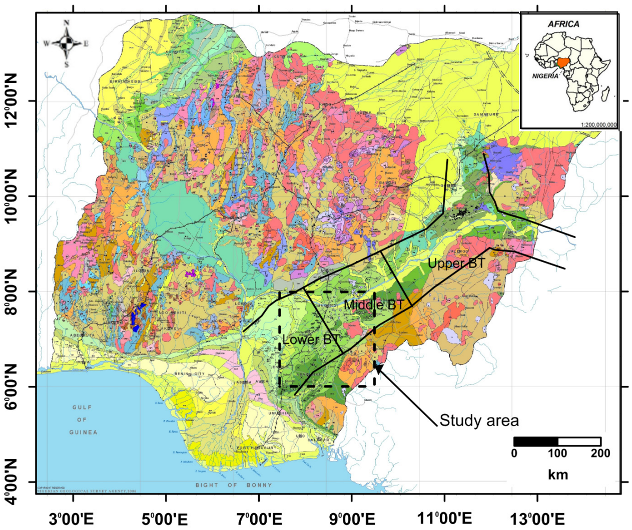

Figure 1. Geological map of Nigeria showing the NE-SW Benue trough, sub-divisions and location of study.

Interpretation of computed Curie depths has been done in terms of the different rock types found in the area [39]. The different basement rock types are; the Precambrian granites and gneisses [36,37,40,41]. Both the Cretaceous and Tertiary-recent sediments have been intruded by igneous intrusions [39].

Anticlinal axes within the sedimentary section have also been identified and interpreted in the region [38,40,42,43]. The intruded igneous rocks (Tertiary volcanic) and the anticlinal axes (Santonian) account for the shallow basement as well as the thinner crust in the region [28,29,31].

3. Data and Methodology

The aeromagnetic data presented in this work are part of the Nigeria's nation-wide high-resolution geophysical data project [36,39]. The high-resolution aeromagnetic data are obtained from the Nigerian Geological Survey Agency (NGSA) flown between 2006 and 2007 by Fugro Airborne Survey. The data acquisition was done on the basis of the dominant NE-SW regional strike (i.e., parallel to the orientation of the Benue trough). The traverse line spacing was set at 500 m and 2 km control line. The data were recorded 80 m above the ground's surface every 0.1 s. Figure 3 shows the reduced-to-the-magnetic-pole (RTP) of the TMI of the area. The RTP is obtained at a geomagnetic inclination of 15°, geomagnetic declination of 2° and amplitude correction of 40 m. On the map, the magnetic highs and lows were identified and interpreted in other reported research [36].

Depth calculation from susceptibility studies based on borehole data is more accurate and reliable [18,44-47]. Scaling of geology from the magnetization point of view showed that power law: $\boldsymbol{\varphi_m(l_x, l_y) \propto l^{-\beta}}$ [48-52], where, $\boldsymbol{\varphi_m}$ stands for

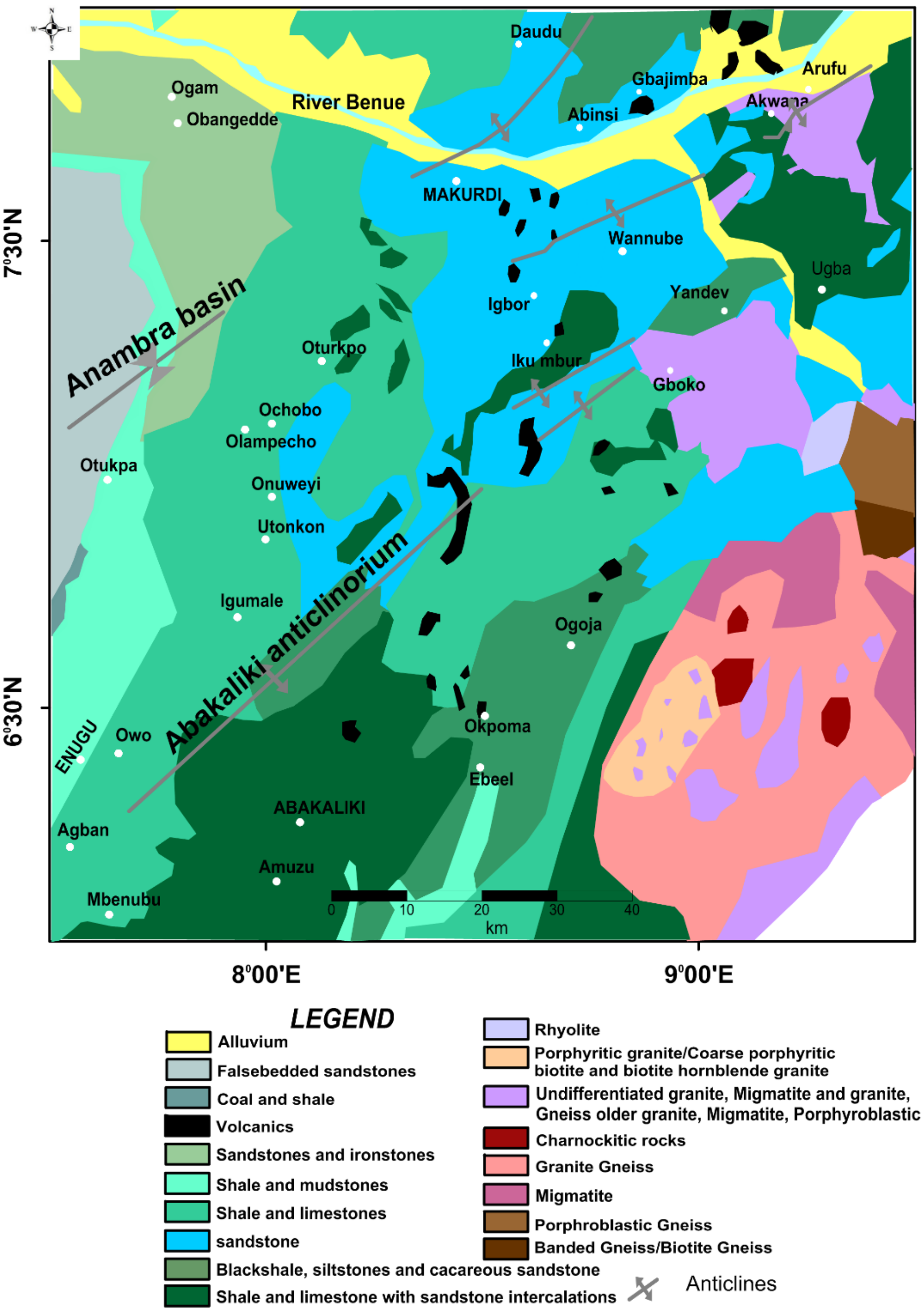

Figure 2. The geology and major structural features (anticlines) 68 of the study area.

magnetization power spectra, $\boldsymbol{l_x}$ and $\boldsymbol{l_y}$ are the wavenumbers in the **x** and **y** directions and their Euclidean norm $\boldsymbol{k} = \sqrt{\boldsymbol{l_x^2 + l_y^2}}$ measured in rad/km, and $\boldsymbol{\beta}$ represents the scaling exponent which described the non-homogeneity of sources in a region [36,47,52].

The top depth ($\boldsymbol{Z_t}$) of an anomalous body in terms of magnetic field ($\boldsymbol{\Phi_t(l)}$) of 1-D radially averaged power spectrum is calculated as follows [7]:

$$\ln\left(\Phi_t(l)\right) = A_1 - 2lZ_t - \beta * \ln(l) \quad (1)$$

where A_1 is a constant.

Whereas, centroid depth ($\boldsymbol{Z_0}$) of the anomalous magnetic body is as follows [8,10]:

$$\ln\left(\frac{\Phi_t(l)}{l^2}\right) = A_2 - 2lZ_0 - \beta * \ln(l) \quad (2)$$

where $\boldsymbol{A_2}$ is a constant, which depends upon the magnetization of source body.

A combination of the two equations was used and computed for the bottom (i.e., Curie) depths ($\boldsymbol{Z_b}$) as follows [2]:

$$Z_b = 2Z_0 - Z_t \quad (3)$$

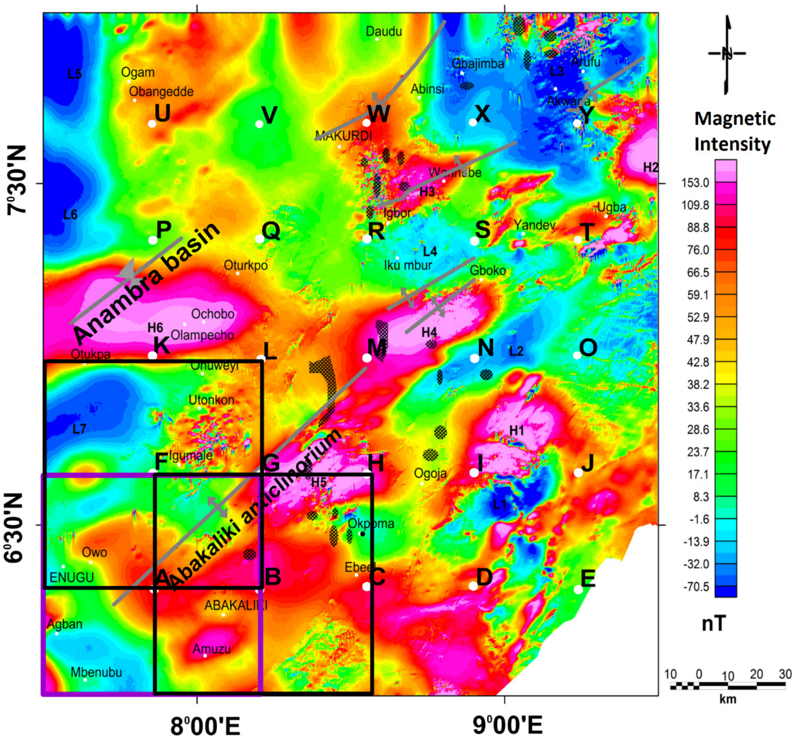

Figure 3. RTP-TMI anomaly map of the study area. Centers of block (A–Y) are shown in white dots for estimation of bottom magnetic (Curie) depths as well as the surface heat flow values (SHF) underneath the study area. Every block is 50% overlapped over the other as shown.

Because of the non-consistency in results of the simultaneous estimation of depths and scaling exponent (**β**) values [17,18,53] using Equations (1) and (2), for which others are of the option that scaling exponent (**β**) be given a constant value for a region of common geology [9,51,52]. Fixed fractal parameter (scaling exponent, **β**) of unity was used [39] on the basis of publication [20] and calculated the top ($\boldsymbol{Z_t}$) depths (km) and centroid ($\boldsymbol{Z_0}$) depths (km) from each of the power spectral blocks (A, B, C, …, Y) of the magnetic anomaly of the study area.

Curie depth (Z_b) results have been used in the estimation of SHF values for the study area [2], using the 1-D Fourier law based on a conductive mode of heat transfer [54]. The Fourier law works where there is no heat transportation by mode of convection, no radiogenic heat and constant temperature gradient (dT/dz). Empirically, the Fourier law [54], can be written as:

$$q_s = k\frac{dT}{dz} \tag{4}$$

where, q_s stands for SHF, k is thermal conductivity (W/m°C) which depends upon the lithology, temperature and pressure. The average thermal conductivity for the region is 2.5 W/m°C [39]. The Curie temperature is written as a function of temperature gradient and Curie depth as follows [54]:

$$\theta_c = \left(\frac{dT}{dz}\right)Z_b \tag{5}$$

From the above Equations (4) and (5), the SHF can be derived as:

$$q_s = \frac{k\theta_c}{Z_b} \tag{6}$$

Here, Curie temperature of $\theta_c = 580°C$ is used in the calculations of SHF in the region.

4. Results and Discussion

Figure 4 shows the power spectrum of block (C) and the calculated top, centroid and bottom depths of magnetic body.

Detailed results of the Curie depths as well as the computed SHF values in all of the blocks (A, B, C, …, Y) are shown in Table 1.

The interpretation of geophysical data because of ambiguity, is usually constrained on the basis of geological formations found in the region or other regions of similar geology/tectonic [29-31,38,40,41,55-58].

Detailed and critical analysis of results shows Curie depths (km) between 11 km and 27 km. Plot of the calculated curie depths between 12 km and 26 km at a 2 km contour interval is as shown (Figure 5). The shallowest depth of 11 km is calculated around the area of Abakaliki (A) whereas the deepest depth was calculated around Otukpa (K). The lowest Curie depth as calculated is related to the Abakaliki anticlinorium while the deepest result is in connection with the Anambra basin. It is stimulating to notice that lower Curie depths are noted over the basement rocks and areas affected by Tertiary volcanic [59,60]. Elucidation of geology and interpretation of geophysical data in the region has shown the animation of underplat-

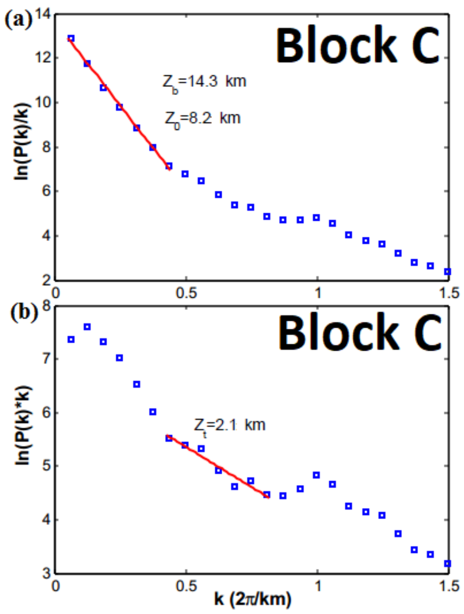

Figure 4. Plots of power spectrums for Block (C) for the bottom (Z_b) and centroid (Z_o) depths (a) and top (Z_t) depth (b) calculations. Best fits for computations of the depths on the spectra are shown (i.e., in red lines).

Table 1. Results of estimated magnetic bottom (Curie) depths surface heat flow (SHF) values for different blocks in the region.

Magnetic Block	Curie Depth (km)	Surface Heat Flow (mWm^{-2})
A	11	132
B	16	91
C	14	104
D	15	97
E	12	121
F	18	81
G	18	81
H	17	85
I	17	85
J	15	97
K	27	54
L	22	66
M	18	81
N	19	76
O	20	72
P	23	63
Q	23	63
R	22	66
S	16	91
T	17	85
U	19	76
V	19	76
W	23	63
X	22	66
Y	18	81

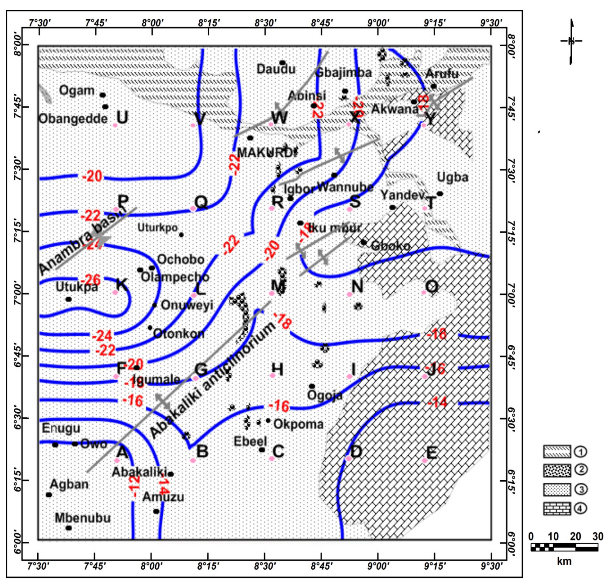

Figure 5. Computed Curie depths (km) underneath the area based on the modified centroid method is presented. The calculated depths are in the range between 11 km and 27 km. The map is prepared based on the overlapping blocks. The legends: (1) is the Tertiary-recent sediments (2) is the Tertiary volcanic (3) is the Cretaceous sediments and (4) is the Precambrian basement rocks.

Table 2. Calculated values of SHF over some major locations in the region.

SHF Status	SHF Values (mWm^{-2})	Block Numbers	Locations
Lower	54	K	Utukpa
	63	P, Q & W	Uturkpo & Makurdi
Intermediate	81	F & G	Akwana & Igumale
	76	U & V	Ogam/Obangedde
	66	L, R & X	Onuweyi, Igbor & Akwana
Higher	132	A	Abakaliki
	91	B & S	Ebeel & Yandev
	104	C	Okpoma
	85	H	Ogoja

ing in the crust underneath the region as the result of past tectonic activity [29-31,40,41].

We presented the lower, intermediate and higher calculated values of SHF in the region of study as shown in Table 2.

The lowest (i.e., in block K) SHF as calculated is along the Anambra basin with the highest (block A) result calculated along the Abakaliki anticlinorium axis (Figure 6). It is observed that the zones of the higher values of SHF are consistent with the areas of magmatic intrusions and basement complexes. The Abakaliki anticlinorium along which the highest result (132 mWm^{-2}) is the area strongly affected by intense tectonic and magmatic activities. Published geology and geophysical data show that the intrusion beneath the Abakaliki anticlinorium is beyond its surface exposure [30,31,38,40,41].

Results of the calculated Curie depths (km) [39] were compared with the previously calculated crustal thickness (Moho depths) in the region. The Moho depths results in the region come from regional gravity and seismological studies [30,55,61-63]. Studies of depths to the major density contrast beneath parts of the Benue trough show that Moho depth of about 24 km was reported around Makurdi [61]. The present study found Curie depth of 22–23 km around the Makurdi area. Along the Abakaliki axis, Moho depths of 10–20 km were reported [31,61-63]. The result is comparable with the calculated Curie depth of 11–20 km along this axis. Along the Anambra axis, Moho depths between 28–34 km were reported from gravity data [61-63] and

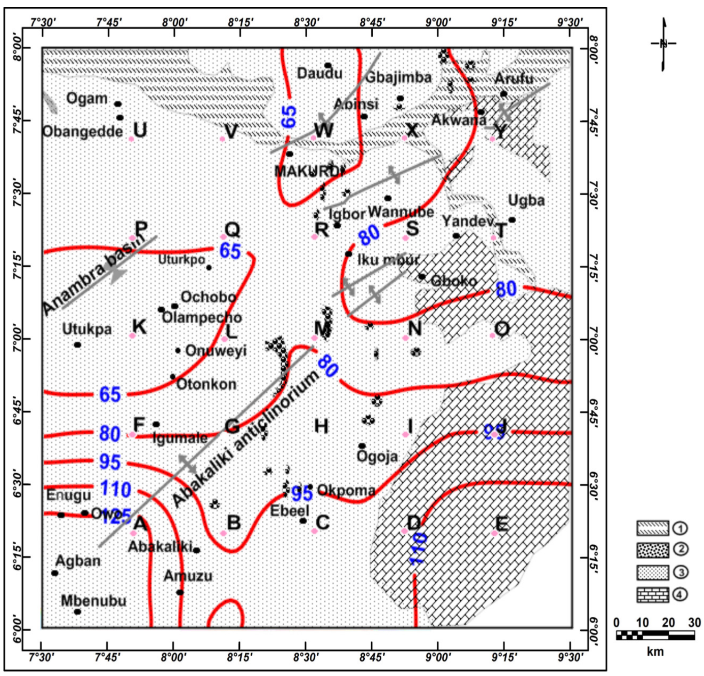

Figure 6. Calculated SHF values in the area based on 1-D Fourier's law. The estimated results in the region are between 54 mWm^{-2} and 132 mWm^{-2}. The map is also prepared by extrapolation to visualize the entire region of the study. The legends: (1) is the Tertiary-recent sediments (2) is the Tertiary volcanic (3) is the Cretaceous sediments and (4) is the Precambrian basement rocks.

Moho depth of 23 km [55] from the broad band seismological station in the region.

The study found the only bore-hole heat flow measurements between 48–76 mWm^{-2} [64-66], in the region from the Anambra basin. In the present study, SHF as calculated along the Anambra basin was between 54–81 mWm^{-2}. The Anambra basin is a rifted subsidiary that formed part of the lower Benue trough. It is of great importance with a high energy-rich in-filled sedimentary thickness of over 9 km [32,38]. In general, it is observed that, with the exception of the Makurdi area where there is surface exposure of Tertiary volcanic, areas where higher SHF values were recorded are consistent with the areas of volcanism and exposed basement rocks. This could indicate that basalts are perhaps deep beneath the sediments around Makurdi. In the region, volcanism intrudes on both the sediments and basement rocks [33]. It is interesting to observe that volcanism in the region is inseparable from the anticlinal folds. In the region, a hot spring (i.e., middle Benue spring) with the highest temperature of around 53.5 °C was recorded [67].

5. Conclusions

This study presents estimation of Curie depth and SHF values in the lower and part of middle Benue trough including part of Anambra basin. The recorded Curie depths in the region vary between 11 km and 27 km. The shallower (11–18 km) Curie depth was interpreted in terms of the Tertiary volcanic and the Precambrian metamorphic (basement) rocks. The computed SHF values are between 54 mWm^{-2} and 132 mWm^{-2} within the study area. Higher SHF (85–132 mWm^{-2}) accounts for the volcanic and metamorphics in the regions. Lower SHF values interpret zones of thick crustal architecture. The results presented are therefore, an attempt towards quantitatively assessing the viability of the thermal energy potentials, extractable of the energy and an installation of a power plant to ascertain the viability of generating electricity from the reservoir.

Author Contributions

Mukaila Abdullahi (MA), Yunis B. Valdon (YBV), Fartisincha P. Andrew (FPA), Bello Yusuf Idi (BYI).

MA, FPA was responsible for project conceptualization, administration, data collection, analysis, literature work, funding acquisition and writing of the original draft of the article. MA, YBV, and BYI were responsible for the geological survey of the study area, data generation, review and final editing. All correspondence is to MA.

Acknowledgments

The author is thankful to the Nigerian Geological Survey Agency (NGSA), Abuja office for providing the aeromagnetic data used in this work. The research was funded by Tertiary Education Trust Fund (TET Fund), Nigeria under the Institutional Based Research (IBR) fund. The authors also acknowledge the Research and Development (R&D) office of Modibbo Adama University Yola, Nigeria through which the research fund was released, and the Departments of Science Laboratory Technology where the research was conducted. The constructive comments and observations of three anonymous reviewers are highly acknowledged.

Conflict of Interest

The authors declared that they have no conflict of interest.

References

[1] Bhattacharyya, B.K., Leu, L.K., 1975. Analysis of magnetic anomalies over Yellowstone National Park: Mapping of Curie point isothermal surface for geothermal reconnaissance. Journal of Geophysical Research. 80, 4461-4465.

[2] Tanaka, A., Okubo, Y., Matsubayashi, O., 1999. Curie point depth based on spectrum analysis of the magnetic anomaly data in East and Southeast Asia. Tectonophysics. 306, 461-470.

[3] Chiozzi, P., Matsushima, J., Okubo, Y., et al., 2005. Curie-point depth from spectral analysis of magnetic data in central-southern Europe. Physics of Earth and Planetary Interior. 152(4), 267-276.

[4] Ross, H.E., Blakely, R.J., Zoback, M.D., 2006. Testing the use of aeromagnetic data for the determination of Curie depth in California. Geophysics. 71, L51-L59.

[5] Rajaram, M., Anand, S.P., Hemant, K., et al., 2009. Curie isotherm map of Indian subcontinent from satellite and aeromagnetic data. Earth and Planetary Science Letter. 281(3-4), 147-158.

[6] Trifonova, P., Zhelev, Z., Petrova, T., et al., 2009. Curie point depths of Bulgarian territory inferred from geomagnetic observations and its correlation with regional thermal structure and seismicity. Tectonophysics. 473(3-4), 362-374.

[7] Bansal, A.R., Gabriel, G., Dimri, V.P., et al., 2011. Estimation of the depth to the bottom of magnetic sources by a modified centroid method for fractal

distribution of sources: an application to aeromagnetic data in Germany. Geophysics. 76, L11-22.

[8] Bansal, A.R., Anand, S.P., Rajaram, M., et al., 2013. Depth to the bottom of magnetic sources (DBMS) from aeromagnetic data of central India using modified centroid method for fractal distribution of sources. Tectonophysics. 603, 155-161.

[9] Bansal, A.R., Dimri, V.P., 2013. Modelling of magnetic data for scaling geology. Geophysical Prospecting. 62(2), 385-396.

[10] Bansal, A.R., Dimri, V.P., Kumar, R., et al., 2016. Curie depth estimation from aeromagnetic for fractal distribution of sources. Fractal solutions for understanding complex system in earth sciences. Springer Earth System Sciences. Springer, Cham: Switzerland. pp. 19-31.

[11] Dunlop, D.J., Ozdemir, O., 1997. Rock magnetism: Fundamentals and frontiers. Cambridge University Press: Cambridge.

[12] Bhattacharyya, B.K., Leu, L.K., 1977. Spectral analysis of gravity and magnetic anomalies due to rectangular prismatic bodies. Geophysics. 42, 41-50.

[13] Shuey, R.T., Schellinger, D.K., Tripp, A.C., et al., 1977. Curie depth determination from aeromagnetic spectra. Geophysical Journal of Royal Astronomical Society. 50, 75-101.

[14] Okubo, Y., Graf, R.J., Hansen, R.O., et al., 1985. Curie point depths of the island of Kyushu and surrounding area, Japan. Geophysics. 50, 481-489.

[15] Blakely, R.J., 1996. Potential theory in gravity and magnetic applications. Cambridge University Press: Cambridge.

[16] Maus, S., Gordon, D., Fairhead, J.D., 1997. Curie temperature depth estimation using a self-similar magnetization model. Geophysical Journal International. 129, 163-168.

[17] Ravat, D., Pignatelli, A., Nicolosi, I., et al., 2007. A study of spectral methods of estimating the depth to the bottom of magnetic sources from near-surface magnetic anomaly data. Geophysical Journal International. 169, 421-434.

[18] Bouligand, C., Glen, J.M.G., Blakely, R.J., 2009. Mapping Curie temperature depth in the western United States with a fractal model for crustal magnetization. Journal of Geophysical Research. 114, B11104.

[19] Ravat, D., Morgan, P., Lowry, A.R., 2016. Geotherms from the temperature-depth-constrained solutions of 1-D steady-state heat-flow equation. Geosphere. 12(4), 1187-1197.

[20] Nwankwo, L.I., 2015. Estimation of depths to the bottom of magnetic sources and ensuing geothermal parameters from aeromagnetic data of Upper Sokoto Basin Nigeria. Geothermics. 54, 76-81.

[21] Melouah, O., Eldosouky, A.M., Ebong, E.D., 2021. Crustal architecture, heat transfer modes and geothermal energy potentials of the Algerian Triassic provinces. Geothermics. 96, 102211.

[22] Onwuemesi, A.G., 1997. One-dimensional spectral analysis of aeromagnetic anomalies and curie depth isotherm in the Anambra basin of Nigeria. Journal of Geodynamics. 23(2), 95-107.

[23] Nwankwo, C.N., Ekine, A.S., Nwosu, L.I., 2009. Estimation of the heat flow variation in the Chad basin, Nigeria. Journal of Applied Sciences and Environmental Management. 13, 73-80.

[24] Obande, G.E., Lawal, K.M., Ahmed, L.A., 2014. Spectral analysis of aeromagnetic data for geothermal investigation of Wikki Warm spring, north-east Nigeria. Geothermics. 50, 85-90.

[25] Abraham, E.M., Obande, E.G., Chukwu, M., et al., 2015. Estimating depth to the bottom of magnetic sources at Wikki warm spring region, northeastern Nigeria, using fractal distribution of sources approach. Turkish Journal of Earth Sciences. 24(5), 494-512.

[26] Chukwu, C.G., Udensi, E.E., Abraham, E.M., et al., 2017. Geothermal energy potential from analysis of aeromagnetic data of part of the Niger-delta basin, southern Nigeria. Energy. 143, 846-853.

[27] Lawal, T.O., Nwankwo, L.I., Iwa, A.A., et al., 2018. Geothermal energy potential of the Chad basin, north-eastern Nigeria. Journal Applied Science and Environmental Management. 22(11), 1817-1824.

[28] Carter, J.D., Barber, W., Tait, E.A., et al., 1963. The geology of parts of Adamawa, Bauchi and Bornu Provinces in northeastern Nigeria. Bulletin of Geological Society of Nigeria. 30, 109.

[29] Cratchley, C.R., Jones, G.P., 1965. An interpretation of the geology and gravity anomalies of the Benue Valley Nigeria. Oversea Geological Survey, Geophysics Paper. (1), 1-25.

[30] Ajayi, C.O., Ajakaiye, D.E., 1981. The origin and perculiarities of the Nigerian Benue Trough: Another look from recent gravity data obtained from middle Benue. Tectonophysics. 80, 285-303.

[31] Adighije, C., 1981. A gravity interpretation of the Benue Trough, Nigeria. Tectonophysics. 79, 109-128.

[32] Agagu, O.K., Adighije, C.I., 1983. Tectonic and sedimentation framework of the lower Benue Trough, southeastern Nigeria. Journal of African Earth Sciences. 1(3/4), 267-274.

[33] Ofoegbu, C.O., 1984. Interpretation of aeromagnetic anomalies over Lower and Middle Benue Trough of Nigeria. Geophysical Journal of Royal Astronomical Society. 79, 813-823.

[34] Benkhelil, J., 1989. The origin and evolution of the Cretaceous Benue Trough (Nigeria). Journal of African Earth Sciences. 6, 251-282.

[35] Ogunmola, J.K., Ayolabi, E.A., Olobaniyi, S.B., 2016. Structural-depth analysis of the Yola Arm of the Upper Benue Trough of Nigeria using high resolution aeromagnetic data. Journal of African Earth Sciences. 124, 32-43.

[36] Abdullahi, M., Kumar, R., Singh, U.K., 2019. Magnetic basement depth from high-resolution aeromagnetic data of parts of lower and middle Benue Trough (Nigeria) using scaling spectral method. Journal of African Earth Sciences. 150, 337-345.

[37] Obaje, N.G., 2009. Geology and mineral resources of Nigeria. Springer: Berlin. pp. 221.

[38] Abdullahi, M., Singh, U.K., 2018. Basement geology derived from gravity anomalies beneath the Benue Trough of Nigeria. Arabian Journal of Geosciences. 11, 694.

[39] Abdullahi, M., Kumar, R., 2020. Curie depth estimated from high-resolution aeromagnetic data of parts of lower and middle Benue trough (Nigeria). Acta Geodaetica et Geophysica. 55(4), 627-643.

[40] Anudu, G.K., Stephenson, R.A., Macdonald, D.I.M., 2014. Using high-resolution aeromagnetic data to recognize and map intra-sedimentary volcanic rocks and geological structures across the Cretaceous middle Benue Trough, Nigeria. Journal of African Earth Sciences. 99, 625-636.

[41] Maluski, H., Coulon, C., Popoff, M., et al., 1995. $40^{Ar}/39^{Ar}$ chronology, petrology and geodynamic setting of Mesozoic to early Cenozoic magmatism from the Benue Trough, Nigeria. Journal of Geological Society, London. 152, 311-326.

[42] Ajayi, C.O., Ajakaiye, D.E., 1986. Structures deduced from gravity data in the middle Benue Trough, Nigeria. Journal of African Earth Sciences. 5(4), 359-369.

[43] Ofoegbu, C.O., 1985. A review of the geology of the Benue Trough, Nigeria. Journal of African Earth Sciences. 3(3), 283-291.

[44] Maus, S., Dimri, V.P., 1996. Depth estimation from the scaling power spectrum of potential fields. Geophysical Journal International. 124, 113-120.

[45] Pilkington, M., Todoeschuck, J.P., 1993. Fractal magnetization of continental crust. Geophysical Research Letter. 20, 627-630.

[46] Pilkington, M., Gregotski, M.E., Todoeschuck, J.P., 1994. Using fractal crustal magnetization models in magnetic interpretation. Geophysical Prospecting. 42, 677-692.

[47] Bansal, A.R., Gabriel, G., Dimri, V.P., 2010. Power law distribution of susceptibility and density and its relation to seismic properties: An example from the German Continental Deep Drilling Program. Journal of Applied Geophysics. 72, 123-128.

[48] Pilkington, M., Todoeschuck, J.P., 1995. Scaling nature of crustal susceptibilities. Geophysical Research Letter. 22, 779-782.

[49] Maus, S., Dimri, V.P., 1994. Scaling properties of potential fields due to scaling sources. Geophysical Research Letter. 21, 891-894.

[50] Maus, S., Dimri, V.P., 1995. Potential field power spectrum inversion for scaling geology. Journal of Geophysical Research. 100, 12605-12616.

[51] Fedi, M., Quarta, T., Santis, A.D., 1997. Inherent power-law behavior of magnetic field power spectra from a Spector and Grant ensemble. Geophysics. 62, 1143-1150.

[52] Kumar, R., Bansal, A.R., Anand, S.P., et al., 2018. Mapping of magnetic basement in Central India from aeromagnetic data for scaling geology. Geophysical Prospecting. 66, 226-239.

[53] Li, C.F., Lu, Y., Wang, J., 2017. A global reference model of Curie-point depths based on EMAG2. Scientific Report. 7(1), 45129.

[54] Turcotte, D.L., Schubert, G., 1982. Geodynamics applications of continuum physics to geologic problems. Wiley: New York.

[55] Akpan, O., Nyblade, A., Okereke, C., et al., 2016. Crustal structure of Nigeria and Southern Ghana, West Africa from P-wave receiver functions. Tectonophysics. 676, 250-260.

[56] Pham, L.T., Eldosouky, A.M., Melouah, O., et al., 2021. Mapping subsurface structural lineaments using the edge filters of gravity data. Journal of King Saud University—Science. 33(8), 101594.

[57] Melouah, O., Pham, L.T., 2021. An improved ILTHG method for edge enhancement of geological structures: Application to gravity data from the Oued Righ valley. Journal of African Earth Sciences. 177, 104162.

[58] Melouah, O., Steinmetz, R.L.L., Ebong, E.D., 2021. Deep crustal architecture of the eastern limit of the West African Craton: Ougarta range and western Algerian Sahara. Journal of African Earth Sciences. 183, 104321.

[59] Tokam, K.A.P., Tabod, C.T., Nyblade, A.A., et al.,

2010. Structure of the crust beneath Cameroon, West Africa, from the joint inversion of Rayleigh wave group velocities and receiver functions. Geophysical Journal International. 183, 1061-1076.

[60] Tugume, S., Nyblade, A., Julià, J., et al., 2013. Precambrian crustal structure in Africa and Arabia: Evidence lacking for secular variation. Tectonophysics. 609, 250-266.

[61] Fairhead, J.D., Okereke, C.S., 1987. A regional gravity study of the West African rift system in Nigeria and Cameroon and its tectonic implication. Tectonophysics. 143, 141-159.

[62] Okereke, C.S., 1988. Contrasting modes of rifting: The Benue Trough and Cameroon volcanic line, West Africa. Tectonics. 7(4), 775-784.

[63] Fairhead, J.D., Okereke, C.S., Nnange, J.M., 1991. Crustal structure of the Mamfe basin, West Africa based on gravity data. Tectonophysics. 186, 351-358.

[64] Nwachukwu, S.O., 1976. Approximate geothermal gradients in the Niger Delta sedimentary basins. The American Association of Petroleum Geology. 60(7), 1073-1077.

[65] Avbovbo, A.A., 1978. Geothermal gradients in the southern Nigerian basins. Bulletin of Canadian Petroleum Geology. 26(2), 268-274.

[66] Onuaha, K.M., Ekine, A.S., 1999. Subsurface temperature variations and heat flow in the Anambra Basin, Nigeria. Journal of African Earth Sciences. 28(3), 641-652.

[67] Kwaya, M.Y., Kurowska, E., 2018. Geothermal exploration in Nigeria—Country update. Proceedings of 7th African Rift Geothermal Conference; 2018 Oct 31; Kigali, Rwanda. Nairobi: ARGeo—The African Rift Geothermal Development Facility.